HHS Public Access

Author manuscript

J Nat Prod. Author manuscript; available in PMC 2017 August 31.

Published in final edited form as:

J Nat Prod. 2016 May 27; 79(5): 1439–1444. doi:10.1021/acs.jnatprod.6b00185.

Characterization of Emodin as a Therapeutic Agent for Diabetic Cataract

Kun-Che Chang[†,‡], **Linfeng Li**[‡], **Theresa M. Sanborn**[†], **Biehuoy Shieh**[†], **Patricia Lenhart**[†], **David Ammar**[†], **Daniel V. LaBarbera**[‡], and **J. Mark Petrash**[*,†,‡]

[†]Department of Ophthalmology, School of Medicine, University of Colorado, Anschutz Medical Campus, Aurora, Colorado 80045, United States

[‡]Department of Pharmaceutical Sciences, Skaggs School of Pharmacy and Pharmaceutical Sciences, University of Colorado, Anschutz Medical Campus, Aurora, Colorado 80045, United States

Abstract

Aldose reductase (AR) in the lens plays an important role in the pathogenesis of diabetic cataract (DC) by contributing to osmotic and oxidative stress associated with accelerated glucose metabolism through the polyol pathway. Therefore, inhibition of AR in the lens may hold the key to prevent DC formation. Emodin, a bioactive compound isolated from plants, has been implicated as a therapy for diabetes. However, its inhibitory activity against AR remains unclear. Our results showed that emodin has good selectively inhibitory activity against AR (IC_{50} = 2.69 ± 0.90 μM) but not other aldo-keto reductases and is stable at 37 °C for at least 7 days. Enzyme kinetic studies demonstrated an uncompetitive inhibition against AR with a corresponding inhibition constant of 2.113 ± 0.095 μM. In *in vivo* studies, oral administration of emodin reduced the incidence and severity of morphological markers of cataract in lenses of AR transgenic mice. Computational modeling of the AR–NADP–emodin ternary complex indicated that the 3-hydroxy group of emodin plays an essential role by interacting with Ser302 through hydrogen bonding in the specificity pocket of AR. All the findings above provide encouraging evidence for emodin as a potential therapeutic agent to prevent cataract in diabetic patients.

Graphical abstract

[*]**Corresponding Author:** Tel (J. M. Petrash): 303-724-0681. Fax: 303-848-5014. mark.petrash@ucdenver.edu.

Notes

The authors declare no competing financial interest.

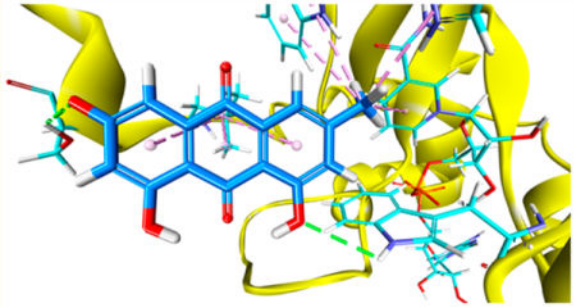

In 2010 approximately 285 million people worldwide had diabetes,[1] and this is predicted to increase to 552 million people by the year 2030.[2] Hyperglycemia in diabetic patients is a robust factor causing organ damage to the eye and kidney, as well as neurological and cardiovascular systems.[3–5] In the eye, diabetes is associated with higher incidence of cataracts, or lens opacities. To date, cataract remains a major cause of blindness in the world.[6–8] Tight glycemic control in diabetic subjects reduces the risk of cataract development,[9] although euglycemia is difficult to achieve in practice.

Aldose reductase (AR; AKR1B1), a member of the aldo-keto reductase superfamily, catalyzes the NADPH-dependent reduction of glucose to its sugar alcohol, sorbitol.[10] A positive correlation between hyperglycemia and AR expression has been observed in many studies[11,12] and shows that AR activation plays a key role in diabetic cataract (DC) formation.[13,14] Indeed, diabetes-dependent increases in AR activity can be found in lenses of a rat model of diabetic cataract.[15] In the polyol pathway, galactose is another substrate metabolized by AR and results in accumulation of galactitol, which accumulates to high levels because it cannot be metabolized by sorbitol dehydrogenase (SDH) and also causes cataract formation.[13] AR inhibitors (ARIs) have been utilized to prevent cataract formation in streptozotocin (STZ)-diabetic animal models[16,17] and galactose-fed rats.[18]

In addition to contributing to the pathogenesis of DC, the action of AR has been linked to other kinds of ocular diseases such as uveitis,[19–21] retinopathy,[11,22] and lens changes associated with posterior capsular opacification.[23,24] Our previous studies indicated that genetic ablation or pharmacological inhibition of AR reduced inflammatory responses in the eye[20,21] and prevented retinal pigment epithelial (RPE) cell death under hyperglycemic conditions.[11] As a result of these observations, blockade of AR appears to be a strategy for prevention of a variety of ocular diseases. Unfortunately, previous clinical trials of ARIs have been unsuccessful due to toxicity and side effects related to poor specificity.[25–27] Therefore, inhibitors with a high degree of specificity toward AR are needed.

Plant-derived compounds have been used for preventing DC for decades;[28] many natural products have been shown to possess AR inhibitory activity and the ability to delay the onset or progression of DC.[29–31] Emodin (1,3,8-trihydroxy-6-methylanthracene-9,10-dione), which is found in many plants,[32,33] has been shown to have a variety of therapeutic effects, such as anti-inflammatory[34] and antidiabetic effects in mouse models.[35–37] While one study showed AR inhibitory activity of emodin *in vitro*,[38] detailed studies of emodin as a therapeutic agent against diabetic eye disease have not been reported. To determine whether

emodin plays a protective role in preventing DC formation, we conducted studies on lens epithelial cells (LECs) and AR transgenic (AR-Tg) mice. We tested the inhibitory activity of emodin against AR *in vitro* by sorbitol accumulation assay. Our results revealed that emodin suppressed sorbitol accumulation and phenotypes associated with DC pathogenesis in AR-Tg mice, suggesting that emodin has potential for use as an ARI and therapeutic agent for the prevention of DC.

RESULTS AND DISCUSSION

Emodin, but Not Chrysophanol Shows Inhibitory Activity against Aldose Reductase

Chrysophanol (also known as chrysophanic acid) and emodin are anthraquinone derivatives differing in structure only at position 3, which is hydroxylated in emodin (Figure 1). We conducted enzyme inhibition studies to determine the inhibitory efficiency of chrysophanol and emodin against AR and related aldo-keto reductases (AKRs). We observed that emodin inhibits human AR with an IC_{50} value of 2.69 ± 0.90 μM (Figure 2A). However, chrysophanol showed no inhibitory activity against AR even at concentrations as high as 100 μM (Figure 2A). We further analyzed the enzyme kinetics of emodin using DL-glyceraldehyde as a model substrate. Analysis revealed an uncompetitive mode of inhibition of emodin against AR with a corresponding inhibition constant (K_i) of 2.113 ± 0.095 μM (Figure 2B).

To investigate their specific activity, we examined the ability of emodin and chrysophanol to inhibit two additional AKRs, namely, AKR1B10 (human small intestine reductase, HSIR) and AKR1A1 (glucuronate reductase, GR). Our results showed that chrysophanol has no inhibitory activity against any of the AKRs tested, while emodin inhibited AKR1B1 but not AKR1B10 or AKR1A1 (Figure 2C). Cytotoxicity testing of emodin in a human lens epithelial cell line (FHL 124) showed that cell viability was substantially reduced at concentrations exceeding 10 μM, which is far above the IC_{50} for enzyme inhibition (Figure 2D). We also measured sorbitol accumulation (the product of glucose reduction by AR) under high glucose conditions with or without emodin. At 5 μM, emodin attenuated high-glucose-induced elevation of sorbitol accumulation, as expected if emodin was capable of inhibiting AR in cells (Figure 2E).

Emodin Is a Thermal-Stable Agent against Aldose Reductase

To study the thermal stability of emodin, we incubated a 1 μM solution of the compound at 37 °C for a week. We found that inhibitory activity is essentially unchanged over this period of time under these incubation conditions (Figure 3). This stability profile is a desirable feature to consider for future development of emodin for human therapy.

Emodin Reduces Vacuole Formation and Lens Opacification in a Mouse Model

We recently generated human AR transgenic (AR-Tg) mice, designated strains PAR37 and PAR39, that express high levels of human AR and develop lens vacuoles similar to that observed in diabetic cataract.[39] In this study, we utilized the PAR37 strain to test the efficacy of orally administered emodin against the development of histological changes in the lens associated with cataract formation. As we showed in a previous publication, AR-Tg strains

PAR37 and PAR39 but not nontransgenic littermates (wild type, WT) spontaneously develop a lens phenotype by P21 characterized by an extensive array of vacuoles in the outer cortical region of the lens.[40] To test the ability of emodin to suppress this AR-dependent lens phenotype, we initiated treatment of P1 pups by including sufficient emodin (dissolved in DMSO) in the drinking water of nursing mothers to deliver a dose of 35 mg/kg to the mother. As a positive AR inhibitor control, we similarly treated a group with sorbinil, a well-characterized orally active ARI previously shown to block DC formation in a variety of animal models.[41] As shown in Figure 4, lenses from WT mice were free from vacuoles regardless of treatment paradigm (Figure 4A–D). However, in AR-Tg mice, extensive vacuoles were observed in the group from nursing mothers whose drinking water included the drug solvent alone (DMSO) (Figure 4E). In contrast, AR-Tg mice nursed by mothers treated with emodin or sorbinil had significantly fewer vacuoles (Figure 4F and G). By measuring the vacuolated cross sectional area in histological sections, we estimated that vacuoles constitute approximately 18% of the lens of P16 AR-Tg mice. Maternal consumption of ARIs reduced vacuolization to 6.3% in emodin- (Figure 4F) and to 3.8% in sorbinil-treated groups (Figure 4G). Surprisingly, if administration of emodin was initiated 3 days prior to birth of the pups, we observed an even better protective effect on reducing vacuolization to 2% (Figure 4H). The effect of drug treatment on vacuolization in the various treatment groups is shown graphically in Figure 4I.

Molecular Modeling Analysis

To understand the structure–activity relationship of emodin and chrysophanol, we conducted molecular docking simulation using the Biovia Discovery Studio 2016 software. Both emodin and chrysophanol were docked into the crystal structure of human AKR1B1 (PDB: 2FZD, resolution 1.08 Å). The binding mode of emodin with human AR revealed that emodin has favorable hydrophobic interactions with Leu300; the 3-hydroxy and the 8-hydroxy group formed a tight hydrogen bond with Ser302 and Trp20 in the specificity pocket, respectively. Moreover, the methyl group also showed a hydrophobic interaction with the side chain of residue His110 and the $NADP^+$ cofactor in the anionic pocket and Trp111 in the specificity pocket (Figure 5A). According to our docking model, the docked emodin was found to have a similar binding pose to β-glucogallin (BGG), a well-characterized selective AR inhibitor,[30,42] sharing the key hydrogen bond interaction with Ser302. In addition, superimposition of docked emodin and BGG suggested that emodin also occupies the binding pocket in a similar fashion (Figure 5B), which could be the reason for the observed similar AR activity. Detailed analysis of the binding pose of emodin indicates that the hydroxyl group at the 3-position of emodin is crucial for its binding with AR. In the case of chrysophanol, these key hydrogen bond interactions were absent because it does not have the corresponding hydroxyl group. We consider this a logical explanation for the observed loss of AR inhibitory activity for chrysophanol and the selective AR inhibition of emodin. Thus, the presence of the 3-hydroxyl group of emodin appears to be essential to its potent biological activity.

CONCLUSIONS

Emodin and chrysophanol are derivatives of anthraquinone that can be found in plants and metabolites of fungi and bacteria.[43–47] Our results build from a previous observation that emodin has inhibitory activity against AR[38] by conducting more *in vivo* and *in vitro* experiments and including a comparative structure–function study of emodin and chrysophanol, a compound with structural similarity to emodin but no detectable AR inhibitory activity (Figure 2A). Indeed, the minor structural difference between chrysophanol and emodin (hydroxyl vs hydrogen at C-3; see Figure 1) appears to determine the difference in inhibitory potency between the two compounds. Many AR inhibitors also block the activity of multiple AKRs such as AKR1B10[48,49] and AKR1A1.[50] To verify the specificity of emodin inhibition, we conducted assays utilizing AKR1B1, AKR1B10, and AKR1A1. As a group, these closely related aldo-keto reductases are similarly capable of reducing reactive aromatic and aliphatic aldehydes. However, AKR1B1 is unique in its ability to catalyze the production of sorbitol, a sugar alcohol linked to the pathogenesis of eye, kidney, and peripheral nerve degeneration associated with diabetes mellitus.[51] Our observation that emodin has a very good specificity for AKR1B1 (Figure 2C) suggests a potential therapeutic role for emodin for prevention of diabetic eye, kidney, and nerve disease without inhibiting the ability of other aldo-keto reductases to protect against aldehyde-mediated toxicity. Computational modeling revealed that emodin likely binds to the AR-NADP(H) binary complex in a manner similar to previously studied AR inhibitors such as BGG (Figure 5B). The key point of inhibitory activity on emodin is its 3-hydroxyl group (absent in chrysophanol), which interacts with Ser302 on AR (Figure 5B), which has been reported as one of the key residues of the AR active site.[52] We can exploit this information to introduce modifications to the emodin structure in order to enhance the specificity and affinity of emodin for the AR binding site. Additionally, the result indicated that emodin is an uncompetitive inhibitor of AR; that is, emodin could bind neither to the substrate-binding region nor to the NADPH-binding region of AR. Moreover, Bohren and Grimshaw conclusively demonstrated that observed noncompetitive to uncompetitive inhibition patterns of ARI can be rationalized in terms of binding of an AR inhibitor to the enzyme–NADP+ complex at the active site, with no need to postulate a alternative catalytic site or allosteric binding site.[53]

Low cytotoxicity (Figure 2D), efficacy in cell line experiments (Figure 2E), and good stability under physiological conditions (Figure 3) led us to examine emodin in an AR-Tg mouse model. *In vivo* studies confirmed the therapeutic effects of emodin on cataract formation using a vacuolization assay (Figure 4). These data support the concept that emodin likely suppresses the cataract phenotype in our animal model via AR inhibition. Further studies will be necessary to explore the possibility that emodin will be efficacious against cataracts resulting from other inciting factors, such as cataracts induced by excessive exposure to UV light.[54]

In addition to AR, emodin also has been shown to inhibit casein kinase II[45] and protein tyrosine kinase,[43] including the nonreceptor tyrosine kinase Src, which has been shown to facilitate stress-related cataract formation and posterior capsular opacification.[55,56] Indeed,

the capability of emodin to inhibit both AR and Src family kinases may provide a dual mode of protection against cataract.

Despite earlier reports that orally administered emodin accumulates to low serum concentrations due to binding to serum proteins,[57,58] we found that treatment of lactating mothers with emodin in drinking water was sufficient to protect against vacuole formation in the lenses of their suckling infant mice. While we did not measure the levels of unbound emodin in maternal or infant blood, we consistently observed its therapeutic effect against lens vacuole formation. This suggests that sufficient quantities of emodin are able to transit the GI tract and gain entry to the lens at concentrations sufficient to affect a phenotypic rescue.

We favor the interpretation that blockade of AR activity is accomplished by the specific interaction of emodin with the active site of AR. In this study, we revealed that enzymatic activity of AR could be blocked by emodin but not chrysophanol (Figure 2). The structural similarity between these two anthraquinones (Figure 1) excludes the nonspecific interaction between emodin and AR. On the contrary, the 3-hydoxy of emodin specifically interacts with Ser302 of AR based on molecular modeling experiments (Figure 5). This data encouraged us to believe that emodin inhibits AR in a pan-assay interference compounds (PAINS)-independent manner.

Many AR inhibitors have been developed as a strategy to prevent or substantially suppress the development of diabetic complications affecting the visual system, peripheral nerves, and kidney. However, several of them such as imirestat,[27] tolrestat,[25,26] and zoporestat[26] were associated with renal and/or liver toxicity and failed in clinical trials. Development of natural compounds as AR inhibitors is an urgent need for treatment of diabetic complications.[59] Foods such as cinnamon[60] and lichens[61] have been reported to contain natural compounds as AR inhibitors. Our previous studies using natural product BGG isolated from Indian gooseberry showed robust inhibitory activity against AR with very low cytotoxicity.[11,20,21] Further studies will be needed to establish the clinical efficacy and safety of emodin, a promising therapeutic sourced primarily from plants.[38,62]

EXPERIMENTAL SECTION

Materials and Cell Culture

Emodin (1,3,8-trihydroxy-6-methylanthracene-9,10-dione) and chrysophanol (1,8-dihydroxy-3-methyl-9,10-anthraquinone) were purchased from Sigma-Aldrich (St. Louis, MO, USA). Sorbinil was generously provided by Pfizer Center Research. Human lens epithelial cells (FHL 124 cell line created by Reddan)[63] were generously provided by Dr. Ram H. Nagaraj (Department of Ophthalmology, University of Colorado Anschutz Medical Campus) and were cultured in low glucose (1 g L^{-1}) Dulbecco's modified Eagle medium (DMEM) supplemented with 4 mM L-glutamine, 5% (v/v) fetal bovine serum, 100 units mL^{-1} penicillin, and 100 μg mL^{-1} streptomycin. Cells were maintained in a humidified incubator containing 5% carbon dioxide at 37 °C.

Animals and Treatments

AR transgenic mice (strain PAR37)[40] and nontransgenic littermate controls were assigned with approximately equal gender distribution to different feeding groups (DMSO, $n = 4$; emodin, $n = 6$; sorbinil, $n = 3$). From the birthdate of pups onward, unless specified otherwise, nursing mothers were given emodin (35 mg kg^{-1}), sorbinil (80 mg kg^{-1}), or vehicle (DMSO) in their drinking water. Where specified, pregnant mice were given emodin (35 mg kg^{-1}) in drinking water for 3 days before pups were born and then continuously afterward. Breeding females were checked daily in order to mark the beginning of pregnancy. Mouse pups were euthanized, and eyes fixed in formalin and embedded with paraffin. Tissue slides were mounted on glass slides and stained with hematoxylin and eosin (H&E). This research was conducted in compliance with the ARVO Statement for the Use of Animals in Ophthalmic and Vision Research. C57BL/6 mice (The Jackson Laboratory) were handled in strict accordance with good animal practice. All animal work was approved by the Institutional Animal Care and Use Committee at the University of Colorado Anschutz Medical Campus.

Aldo-keto Reductases

Recombinant human AKR1B1, AKR1B10, and AKR1A1 were purified from *E. coli* host cultures as described previously.[64] Enzyme solutions were stored at −80 °C and, when thawed, were maintained at 4 °C before use. AKR activity was determined spectrophotometrically by measuring the decrease in absorbance at 340 nm upon oxidation of NADPH.[42] Reaction mixtures in 1.0 mL quartz cuvettes contained DL-glyceraldehyde (1.0 mM for AKR1B1, 25 mM for AKR1B10, and 15 mM for AKR1A1) and 150 μM NADPH in KAB buffer (50 mM HEPES, pH 7.5, 150 mM NaCl, 1 mM DTT, 10 mM $MgCl_2$). For kinetics studies, rates were measured in triplicate under varying substrate and inhibitors (emodin and chrysophanol) concentrations. Rate and inhibition constants were compared using GraphPad Prism (San Diego, CA, USA).

Cell Viability and Sorbitol Colorimetric Assay

FHL 124 cells (10^4 cells) were grown in 96-well plates for the cell viability assay or 10^5 cells in 60 mm dishes for the sorbitol colorimetric assay. For the viability assay, cells were treated with the indicated concentrations of emodin. After a 24 h treatment, 10 μL of MTT (5 mg mL^{-1} in PBS) was added to 100 μL of culture medium/well for 4 h, and the cell viability was determined by using 3-(4,5-dimethylthiazol-2-yl)-2,5-diphenyltetrazolium bromide (MTT) (Sigma-Aldrich) as described.[65] Levels of MTT were determined by measuring the absorbance at 570 nm by using a BioTek Synergy 4 Hybrid microplate reader (BioTek, Winooski, VT, USA). For sorbitol colorimetric assays, cells were treated with emodin and low or high glucose, followed by washing with cold PBS twice. In lens organ culture, lenses were homogenized using RIPA buffer. The cell lysates were followed by deproteinization with a deproteinizing sample preparation kit (BioVision, Milpitas, CA, USA). Sorbitol determinations with neutralized samples were carried out using a D-sorbitol colorimetric assay kit (BioVision) and a BioTek Synergy 4 hybrid microplate reader for measuring analyte absorbance at 560 nm.

Molecular Docking of Emodin and Chrysophanol with Human AKR1B1

Computational modeling was carried out using the flexible docking protocol of Biovia Discovery Studio 2016. The CHARMm force field was applied to the 1.08 Å AKR1B1 (PDB: 2FZD) crystal structure, water molecules were removed, and residues were corrected for physiological pH. The receptor was minimized by the Smart Minimizer algorithm, an algorithm that performs 1000 steps of steepest descent with a root-mean-square gradient tolerance of 3. The binding site was defined as whole residues within an 8 Å radius subset encompassing the active site. All ligands were prepared and typed with the CHARMm force field before docking studies. LibDock was used to filter the confirmation of the substrates. The number of specified hot spots was set at 100, and max hits to save was set at 10 for each ligand using the "BEST" algorithm for conformational sampling. The top poses of each ligand were selected for flexible docking by using the corresponding protocol in Discovery Studio 2016 that allows for receptor flexibility. The flexible residues were determined to be those in the anionic pocket (Asp43, Tyr48, Lys77, His 110, Phe115 Ser159, Asn160, Gln183, and Tyr209) and specificity pocket (Trp20, Trp79, Trp111, Thr113, Phe122, Pro218, Trp219, Val297, Cys298, Ala299, Leu300, Ser302, and Cys303).[52] Simulated annealing between 300 and 700 K and postdocking ChiRotor refinement were allowed.

Statistical Analysis

Results are shown as the means ± SEM of at least three experiments. Data were analyzed by Student's *t* test with a p value of <0.05 considered significant.

Acknowledgments

This study is supported by NIH grants EY005856 (J.M.P.) and EY021498 (D.V.L. and J.M.P.).

References

1. Vos T, Flaxman AD, Naghavi M, Lozano R, Michaud C, et al. Lancet. 2012; 380(9859):2163–96. [PubMed: 23245607]
2. International-Diabetes-Federation. IDF Diabetes Atlas. 7th. Brussels, Belgium: 2015. p. 1-144.
3. Abdo S, Shi Y, Otoukesh A, Ghosh A, Lo CS, et al. Diabetes. 2014; 63:3483–3496. [PubMed: 24812425]
4. Huang JY, Li LT, Wang H, Liu SS, Lu YM, et al. CNS Neurosci Ther. 2014; 20:816–822. [PubMed: 24712523]
5. Rubin J, Matsushita K, Ballantyne CM, Hoogeveen R, Coresh J, et al. J Am Coll Cardiol. 2012; 59(5):484–9. [PubMed: 22281251]
6. Klein BE, Klein R, Wang Q, Moss SE. Ophthalmic Epidemiol. 1995; 2(1):49–55. [PubMed: 7585233]
7. Rowe NG, Mitchell PG, Cumming RG, Wans JJ. Ophthalmic Epidemiol. 2000; 7(2):103–14. [PubMed: 10934461]
8. Leske MC, Wu SY, Hennis A, Connell AM, Hyman L, et al. Ophthalmology. 1999; 106(1):35–41. [PubMed: 9917778]
9. UK Prospective Diabetes Study (UKPDS) Group. Intensive blood-glucose control with sulphonylureas or insulin compared with conventional treatment and risk of complications in patients with type 2 diabetes (UKPDS 33). Lancet. 1998; 352(9131):837–53. DOI: 10.1016/S0140-6736(98)07019-6 [PubMed: 9742976]
10. Petrash JM, et al. Mol Life Sci. 2004; 61(7–8):737–49.

11. Chang KC, Snow A, LaBarbera DV, Petrash JM. Chem-Biol Interact. 2015; 234:254–60. [PubMed: 25451566]
12. Henry DN, Del Monte M, Greene DA, Killen PD. J Clin Invest. 1993; 92(2):617–23. [PubMed: 8349800]
13. Kador PF. Med Res Rev. 1988; 8(3):325–52. [PubMed: 3136278]
14. Lee AY, Chung SK, Chung SS. Proc Natl Acad Sci USA. 1995; 92(7):2780–4. [PubMed: 7708723]
15. Thiraphatthanavong P, Wattanathorn J, Muchimapura S, Thukham-mee W, Lertrat K, et al. Oxid Med Cell Longevity. 2014; 2014:789406.
16. Kawakubo K, Mori A, Sakamoto K, Nakahara T, Ishii K. Biol Pharm Bull. 2012; 35(6):866–72. [PubMed: 22687477]
17. Matsumoto T, Ono Y, Kuromiya A, Toyosawa K, Ueda Y, et al. J Pharmacol Sci. 2008; 107(3): 340–8. [PubMed: 18612195]
18. Kador PF, Randazzo J, Babb T, Koushik K, Takamura Y, et al. J Ocul Pharmacol Ther. 2007; 23(2): 116–23. [PubMed: 17444799]
19. Yadav UC, Srivastava SK, Ramana KV. Invest Ophthalmol Visual Sci. 2007; 48(10):4634–42. [PubMed: 17898287]
20. Chang KC, Laffin B, Ponder J, Enzsoly A, Nemeth J, et al. Chem-Biol Interact. 2013; 202(1–3): 283–7. [PubMed: 23247009]
21. Chang KC, Ponder J, Labarbera DV, Petrash JM. Invest Ophthalmol Visual Sci. 2014; 55(5):2853–61. [PubMed: 24677107]
22. Tang J, Du Y, Petrash JM, Sheibani N, Kern TS. PLoS One. 2013; 8(4):e62081. [PubMed: 23614016]
23. Chang KC, Petrash JM. Invest Ophthalmol Visual Sci. 2015; 56(8):4198–210. [PubMed: 26132779]
24. Yadav UC, Ighani-Hosseinabad F, van Kuijk FJ, Srivastava SK, Ramana KV. Invest Ophthalmol Visual Sci. 2009; 50(2):752–9. [PubMed: 19011011]
25. Chalk C, Benstead TJ, Moore F. Cochrane Database Syst Rev. 2007; (4):CD004572. [PubMed: 17943821]
26. Gabbay KH. Curr Diabetes Rep. 2004; 4(6):405–8.
27. Suzen S, Buyukbingol E. Curr Med Chem. 2003; 10(15):1329–52. [PubMed: 12871133]
28. West AL, Oren GA, Moroi SE. Am J Ophthalmol. 2006; 141(1):157–66. [PubMed: 16386992]
29. Shin KH, Lim SS, Kim DK. Phytomedicine. 1998; 5(2):121–7. [PubMed: 23195764]
30. Puppala M, Ponder J, Suryanarayana P, Reddy GB, Petrash JM, et al. PLoS One. 2012; 7(4):e31399. [PubMed: 22485126]
31. Shin KH, Kang SS, Kim HJ, Shin SW. Phytomedicine. 1994; 1(2):145–7. [PubMed: 23195888]
32. Gautam R, Karkhile KV, Bhutani KK, Jachak SM. Planta Med. 2010; 76(14):1564–9. [PubMed: 20379952]
33. Nsonde Ntandou GF, Banzouzi JT, Mbatchi B, Elion-Itou RD, Etou-Ossibi AW, et al. J Ethnopharmacol. 2010; 127(1):108–11. [PubMed: 19799981]
34. Ghosh S, Das Sarma M, Patra A, Hazra B. J Pharm Pharmacol. 2010; 62(9):1158–66. [PubMed: 20796195]
35. Wang J, Huang H, Liu P, Tang F, Qin J, et al. Eur J Pharmacol. 2006; 553(1–3):297–303. [PubMed: 17074319]
36. Wang YJ, Huang SL, Feng Y, Ning MM, Leng Y. Acta Pharmacol Sin. 2012; 33(9):1195–203. [PubMed: 22922341]
37. Zhao XY, Qiao GF, Li BX, Chai LM, Li Z, et al. Clin Exp Pharmacol Physiol. 2009; 36(1):29–34. [PubMed: 18785977]
38. Jang DS, Lee GY, Kim YS, Lee YM, Kim CS, et al. Biol Pharm Bull. 2007; 30(11):2207–10. [PubMed: 17978503]
39. Snow A, Shieh B, Chang KC, Pal A, Lenhart P, et al. Chem-Biol Interact. 2015; 234:247–53. [PubMed: 25541468]

40. Zablocki GJ, Ruzycki PA, Overturf MA, Palla S, Reddy GB, et al. Chem-Biol Interact. 2011; 191(1–3):351–6. [PubMed: 21329682]
41. Datiles MB 3rd, Fukui H. Curr Eye Res. 1989; 8(3):233–7. [PubMed: 2523284]
42. Li L, Chang KC, Zhou Y, Shieh B, Ponder J, et al. J Med Chem. 2014; 57(1):71–7. [PubMed: 24341381]
43. Jayasuriya H, Koonchanok NM, Geahlen RL, McLaughlin JL, Chang CJ. J Nat Prod. 1992; 55(5): 696–8. [PubMed: 1517743]
44. Chang CH, Lin CC, Yang JJ, Namba T, Hattori M. Am J Chin Med. 1996; 24(2):139–42. [PubMed: 8874670]
45. Yim H, Lee YH, Lee CH, Lee SK. Planta Med. 1999; 65(1):9–13. [PubMed: 10083837]
46. Bringmann G, Irmer A, Feineis D, Gulder TA, Fiedler HP. Phytochemistry. 2009; 70(15–16):1776–86. [PubMed: 19786287]
47. Liu SY, Lo CT, Chen C, Liu MY, Chen JH, et al. J Biochem Biophys Methods. 2007; 70(3):391–5. [PubMed: 17067682]
48. Cousido-Siah A, Ruiz FX, Crespo I, Porte S, Mitschler A, et al. Chem-Biol Interact. 2015; 234:290–6. [PubMed: 25532697]
49. Zhang L, Zhang H, Zhao Y, Li Z, Chen S, et al. FEBS Lett. 2013; 587(22):3681–6. [PubMed: 24100137]
50. Carbone V, Giglio M, Chung R, Huyton T, Adams J, et al. Eur J Med Chem. 2010; 45(3):1140–5. [PubMed: 20036445]
51. Petrash JM. Cell Mol Life Sci. 2004; 61(7–8):737–749. [PubMed: 15094999]
52. Maccari R, Ottana R. J Med Chem. 2015; 58(5):2047–67. [PubMed: 25375908]
53. Bohren KM, Grimshaw CE. Biochemistry. 2000; 39(32):9967–74. [PubMed: 10933817]
54. Galichanin K, Lofgren S, Soderberg P. Health Phys. 2014; 107(6):523–9. [PubMed: 25353237]
55. Zhou J, Menko AS. Invest Ophthalmol Vis Sci. 2002; 43(7):2293–300. [PubMed: 12091430]
56. Walker JL, Wolff IM, Zhang L, Menko AS. Invest Ophthalmol Visual Sci. 2007; 48(5):2214–23. [PubMed: 17460282]
57. Liang JW, Hsiu SL, Wu PP, Chao PD. Planta Med. 1995; 61(5):406–8. [PubMed: 7480199]
58. Fabriciova G, Sanchez-Cortes S, Garcia-Ramos JV, Miskovsky P. Biopolymers. 2004; 74(1–2): 125–30. [PubMed: 15137109]
59. Galuppo M, Giacoppo S, Bramanti P, Mazzon E. Molecules. 2014; 19(3):2877–95. [PubMed: 24603557]
60. Saraswat M, Muthenna P, Suryanarayana P, Petrash JM, Reddy GB. Asia Pac J Clin Nutr. 2008; 17(4):558–65. [PubMed: 19114390]
61. Raj PS, Prathapan A, Sebastian J, Antony AK, Riya MP, et al. Nat Prod Res. 2014; 28(18):1480–4. [PubMed: 24735436]
62. Kosalec I, Kremer D, Locatelli M, Epifano F, Genovese S, et al. Food Chem. 2013; 136(2):335–41. [PubMed: 23122067]
63. Wormstone IM, Tamiya S, Marcantonio JM, Reddan JR. Invest Ophthalmol Vis Sci. 2000; 41(13): 4216–22. [PubMed: 11095618]
64. Nakano T, Petrash JM. Biochemistry. 1996; 35(34):11196–202. [PubMed: 8780524]
65. Chang KC, Lo CW, Fan TC, Chang MD, Shu CW, et al. BMC Cell Biol. 2010; 11:6. [PubMed: 20089176]

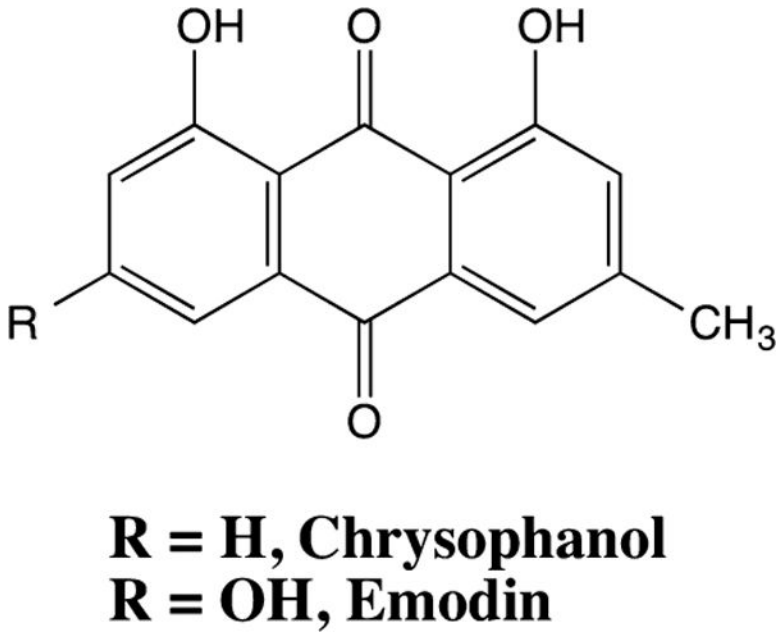

Figure 1.
Structure of emodin and chrysophanol.

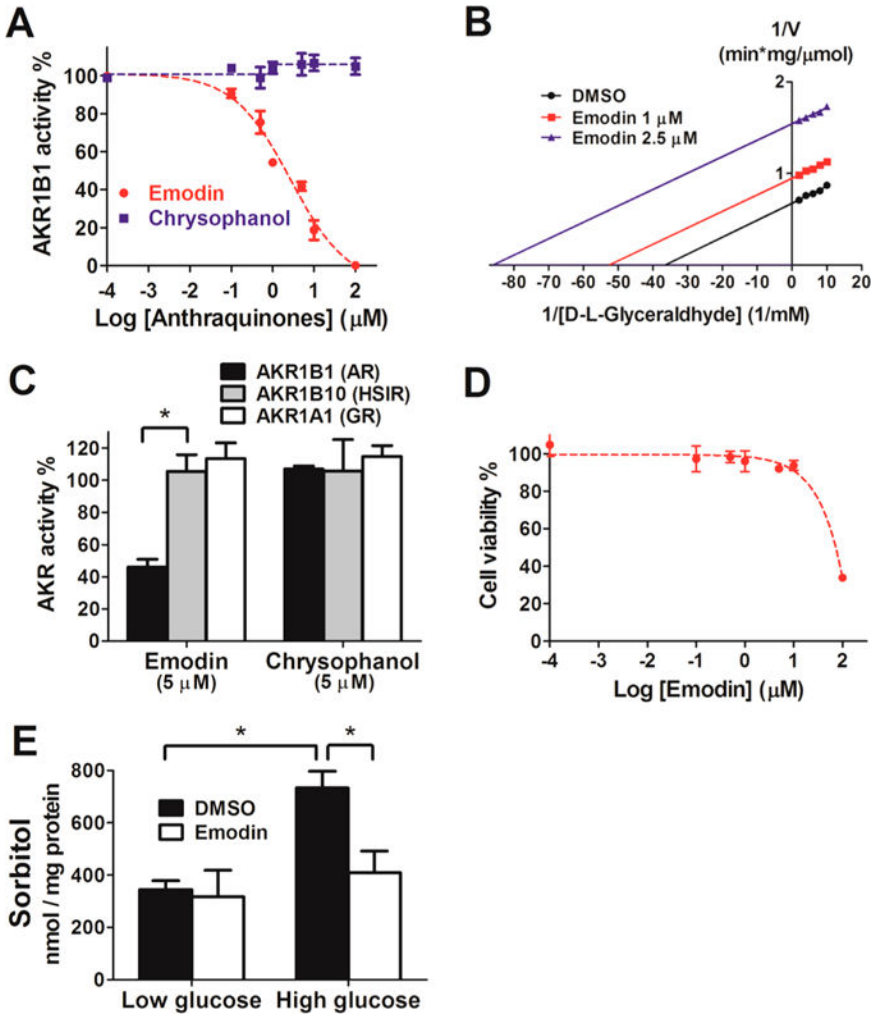

Figure 2.

Inhibitory activity of anthraquinones. (A) The IC_{50} of emodin and chrysophanol against AKR1B1 was determined in the presence of various dosages from 0.1 to 100 μM. (B) Double reciprocal plots of the initial enzyme velocity versus the concentration of substrate in the presence of different concentrations (0, 1, 2.5 μM) of emodin. (C) The inhibitory activity of emodin and chrysophanol against AKR1B1 (aldose reductase, AR), AKR1B10 (human small intestine reductase, HSIR), and AKR1A1 (glucuronate reductase, GR) was measured using DL-glyceraldehyde as the aldehyde substrate as described in the Experimental Section. (D) FHL 124 cells were treated with various concentrations of emodin for 24 h, and cell viability was determined by the MTT assay. (E) AR inhibitory activity in human lens epithelial cells was confirmed utilizing a sorbitol accumulation assay in FHL 124 cells. Cells were treated with emodin (5 μM) and low (5 mM) or high (30 mM) glucose for 24 h. The amount of sorbitol in cell lysates was normalized to total protein. Data shown are means ± SEM ($n = 3$). *$p < 0.05$.

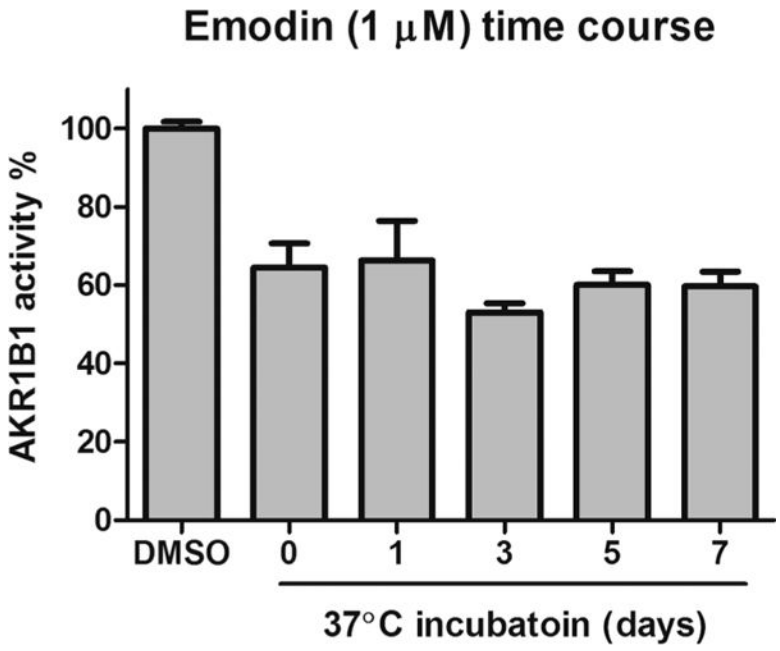

Figure 3.

Stability study of emodin. Emodin (1 μM, in DMSO) was incubated at 37 °C for 1, 3, 5, and 7 days, and its inhibitory activity against AKR1B1 was measured. Data shown are means ± SEM (n = 3).

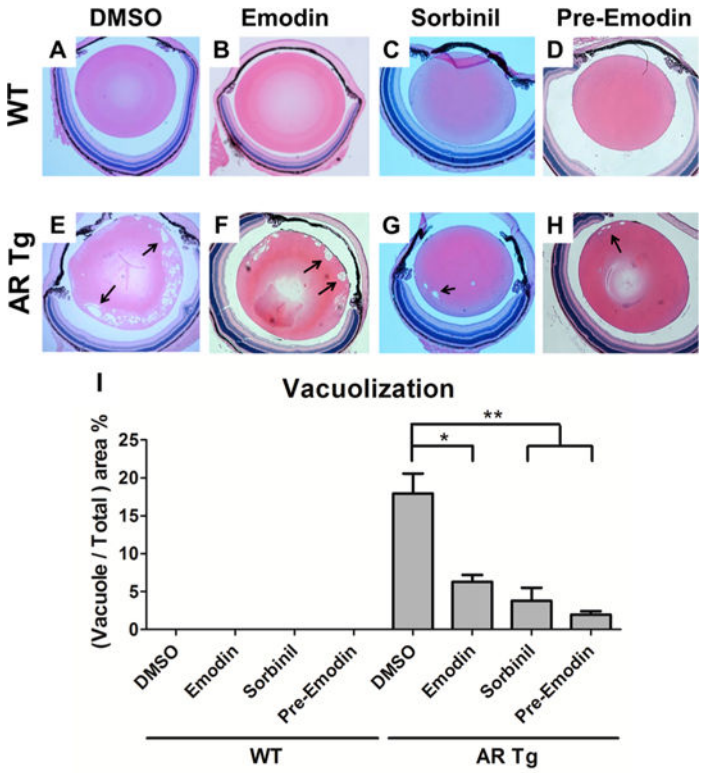

Figure 4.

AR inhibition rescues vacuolization in AR-overexpressed lenses. Nursing dams of newborn WT (A–D) or AR Tg mice (E–H) were treated with DMSO (A, E), emodin (B, F), or sorbinil (C, G) for 16 days or for 3 additional days' treatment with emodin prior to birth (Pre-emodin) (D, H). Percentage of lens cross sectional area covered with vacuoles in each group (I). Histological sections were stained with hematoxylin and eosin (H&E). Arrows indicate vacuoles in lenses. All photomicrographs were taken at 40× magnification. Images are typical of multiple different animals ($n = 3–5$) from each group. Data shown are means ± SEM ($n = 3–5$). *$p < 0.05$; **$p < 0.01$.

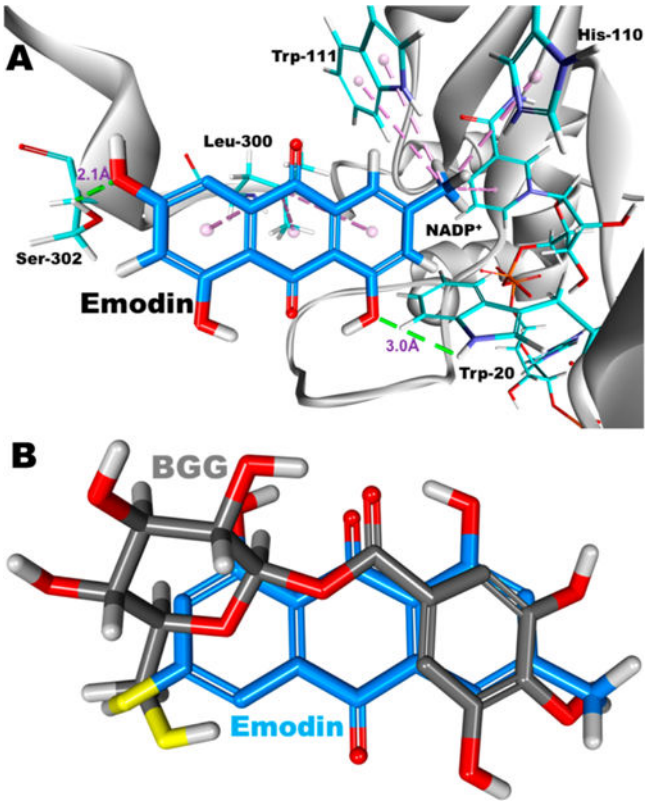

Figure 5.

Molecular modeling of emodin with aldose reductase. (A) Binding model of emodin (blue carbon skeleton) as revealed from flexible docking in the binding site of human AKR1B1. The green dashed lines represent hydrogen bonds, and pink dashed lines represent hydrophobic interactions. (B) Superimposition of docked pose of emodin (blue carbon skeleton) and selective AR inhibitor BGG (gray carbon skeleton). The key hydroxyl groups that interact with Ser302 are highlighted in yellow.